

Supporting Information

Thermogravimetric and spectroscopic analyses, along with the kinetic modeling, of the pyrolysis of phosphate tailings

Xue-Mei Yuan^a, Hui-Juan Xie^a, Deng-Pan Nie^{a,*}, Yu Zhang^{b,*}, Lan Zhou^{a,c}, Yi-Yi Wu^a and Zhu Wen^a

*Corresponding Author: Deng-Pan Nie

E-mail: ndpz@sina.com

Postal address: School of Chemical Engineering, Guizhou Minzu University, Guiyang, China

Telephone number: +86 13339619988

*Corresponding Author: Yu Zhang

E-mail: 342114915@qq.com

Postal address: College of Chemistry and Chemical Engineering, Guizhou University, Guiyang, China

Telephone number: +86 13368515556

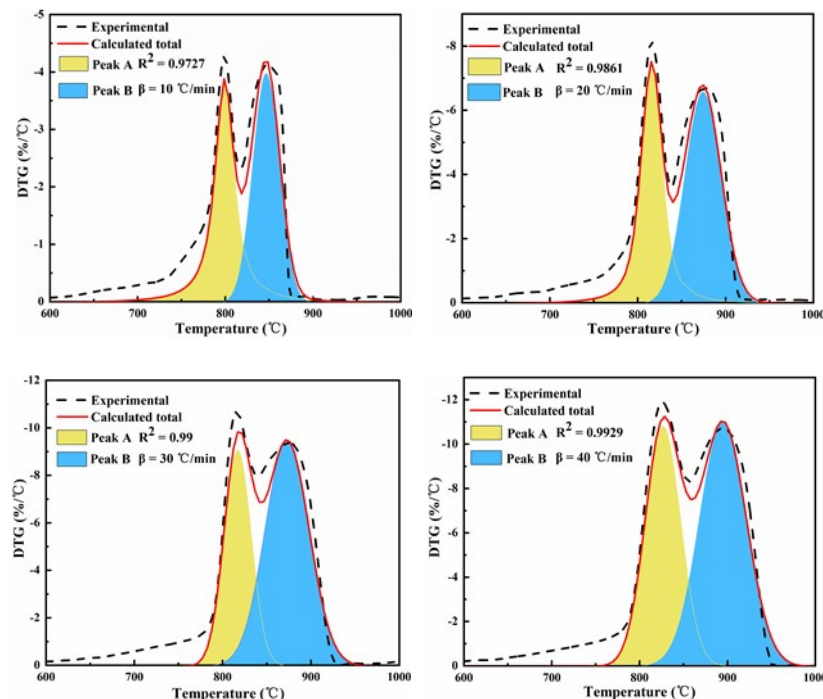


Fig. S1. Optimization of the decomposition process of phosphate tailings at different heating rates.

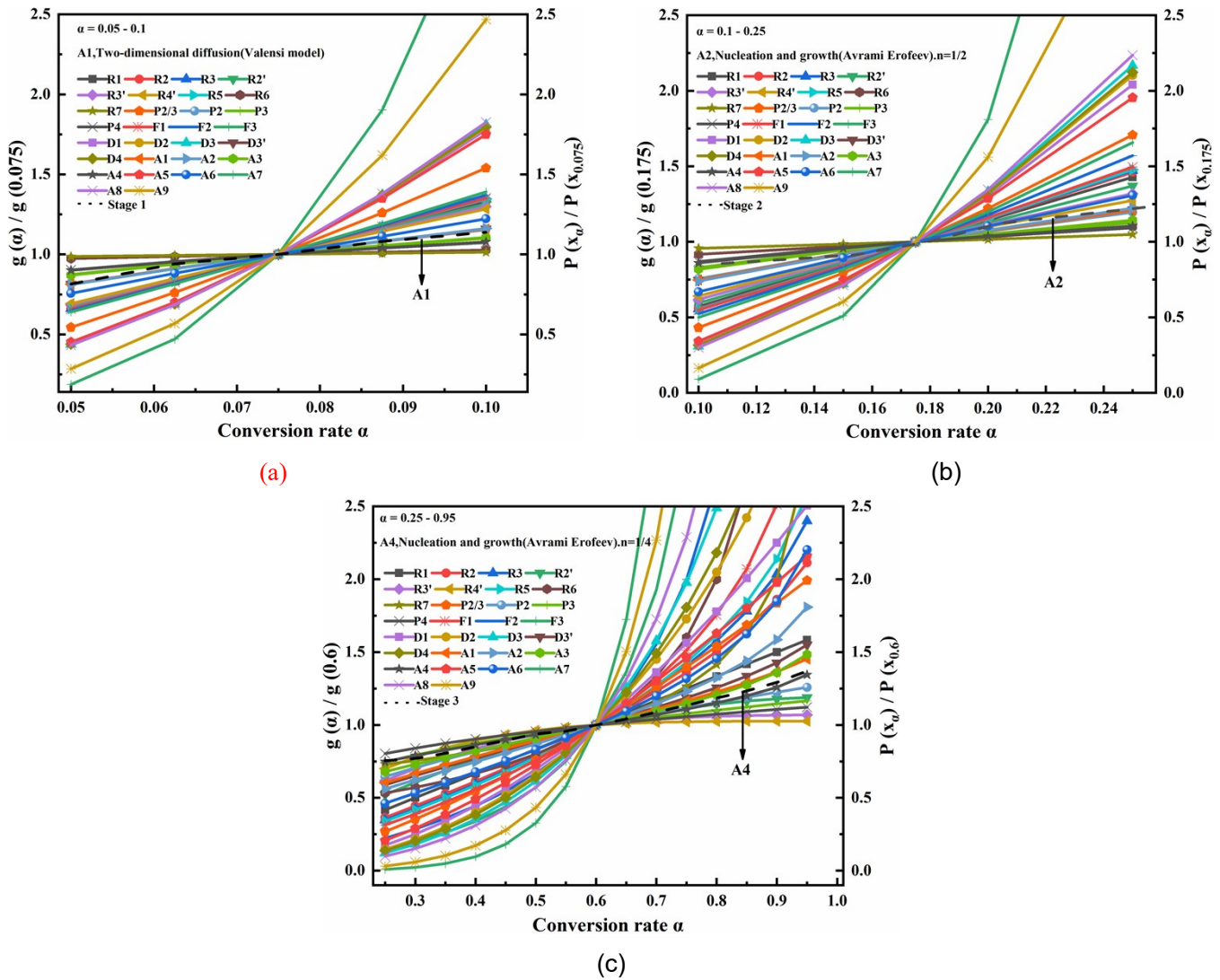


Fig. S2. Analysis of the thermal degradation mechanism of phosphate tailings at different conversion rates by the Criado method.

Table S.1: Common mechanism functions of solid phase reaction.

Reaction model	Symbol	Integral form $g(\alpha)$
Phase boundary-controlled reaction (one-dimensional movement)	R1	α
Phase boundary-controlled reaction (contracting area)	R2	$1 - (1 - \alpha)^{1/2}$
Phase boundary-controlled reaction (contracting volume)	R3	$1 - (1 - \alpha)^{1/3}$
reaction stage	R2'	$1 - (1 - \alpha)^2$
reaction stage	R3'	$1 - (1 - \alpha)^3$
reaction stage	R4'	$1 - (1 - \alpha)^4$
reaction stage	R5	$1 - (1 - \alpha)^{1/4}$
Chemical reaction (second level)	R6	$(1 - \alpha)^{-1}$
Chemical reaction (level 2/3)	R7	$(1 - \alpha)^{-1/2}$
Power low	P2/3	$\alpha^{3/2}$
Power low	P2	$\alpha^{1/2}$
Power low	P3	$\alpha^{1/3}$
Power low	P4	$\alpha^{1/4}$
First order	F1	$-\ln(1 - \alpha)$
Second order	F2	$-1 + (1 - \alpha)^{-1}$
Third order	F3	$1/2([1 - \alpha]^{-2} - 1)$
One-dimensional diffusion	D1	α^2
Two-dimensional diffusion (Valensi model)	D2	$(1 - \alpha)\ln(1 - \alpha) + \alpha$
Three-dimensional diffusion (Jander model)	D3	$(1 - [1 - \alpha]^{1/3})^2$
Three-dimensional diffusion (Jander model)	D3'	$(1 - [1 - \alpha]^{1/3})^{1/2}$
Three-dimensional diffusion (Ginstlinge-Brounshtein model)	D4	$(1 - 2/3\alpha) - (1 - \alpha)^{2/3}$
Two-dimensional diffusion (Valensi model)	A1	$(1 - [1 - \alpha]^{1/2})^{1/2}$
Nucleation and growth (Avrami–Erofeev, $n = 1/2$)	A2	$-\ln(1 - \alpha)^{1/2}$
Nucleation and growth (Avrami–Erofeev, $n = 1/3$)	A3	$-\ln(1 - \alpha)^{1/3}$
Nucleation and growth (Avrami–Erofeev, $n = 1/4$)	A4	$-\ln(1 - \alpha)^{1/4}$
Three-dimensional diffusion (Jander model)	A5	$([1 + \alpha]^{1/3} - 1)/2$
Nucleation and growth (Avrami–Erofeev, $n = 2/3$)	A6	$-\ln(1 - \alpha)^{2/3}$
Nucleation and growth (Avrami–Erofeev, $n = 4$)	A7	$-\ln(1 - \alpha)^4$
Nucleation and growth (Avrami–Erofeev, $n = 2$)	A8	$-\ln(1 - \alpha)^2$
Nucleation and growth (Avrami–Erofeev, $n = 3$)	A9	$-\ln(1 - \alpha)^3$

Table S.2: Possible reaction equations in the pyrolysis process of phosphate tailings.

Equation	T/ΔG	Number
$\text{CaMg}(\text{CO}_3)_2(\text{s}) = \text{CaCO}_3(\text{s}) + \text{MgO}(\text{s}) + \text{CO}_2(\text{g})$	T = 500°C ΔG <0	(1)
$\text{CaCO}_3(\text{s}) = \text{CaO}(\text{s}) + \text{CO}_2(\text{g})$	T = 900°C ΔG <0	(2)
$\text{SiO}_2(\text{s}) + 6\text{HF}(\text{g}) = \text{H}_2\text{SiF}_6 + 2\text{H}_2\text{O}(\text{l})$	T = 300°C ΔG >0	(3)
$\text{H}_2\text{SiF}_6 = \text{SiF}_4(\text{g}) + 2\text{HF}(\text{g})$	T = 200°C ΔG <0	(4)
$\text{CaF}_2 + \text{H}_2\text{SiF}_6 = \text{CaSiF}_6 + 2\text{HF}(\text{g})$	T = 600°C ΔG <0	(5)
$\text{CaO}(\text{s}) + 2\text{HF}(\text{g}) = \text{CaF}_2 + \text{H}_2\text{O}(\text{l})$	T = 0°C ΔG <0	(6)
$2\text{Ca}_5(\text{PO}_4)_3\text{F} = 3\text{Ca}_3(\text{PO}_4)_2 + \text{CaF}_2$	T = 0°C ΔG >0	(7)
$2\text{CaO} + \text{SiO}_2 = \text{Ca}_2\text{SiO}_4$	T = 0°C ΔG <0	(8)
$3\text{CaO} + \text{SiO}_2 = \text{Ca}_3\text{SiO}_5$	T = 0°C ΔG <0	(9)